Chapter 4

Experimental Procedures

In this chapter, the fabrication of the target and preparation of Ga-doped ZnO thin films are described. The method of characterization and analysis of the thin film properties, i.e. structural, electrical and optical properties, are also discussed in details.

4.1 Fabrication of Ga-doped ZnO Target

Ga-doped ZnO (GZO) targets were prepared by sintering the mixture of ZnO powder (purity of 99.999%) [Alfa Aesar^R] and Ga_2O_3 powder (purity of 99.99%) [Alfa Aesar^R] which were separately calcined in a furnace at 900 °C for 3 hrs. After a complete cool down process, the ZnO powder was mixed with varying Ga_2O_3 content in a weight percent of the whole target. The mixture was then blended and rolled in order to obtain fine powder.

In the next step, deionized water (DI-water) was added approximately 10 cc in the mixture for a wet compressing. In this process, the mixture was in a 5 cm in diameter carbon coated mold. The mixed powder was pressed and held under a force of 5.5-6 tons for about 50 minutes in air at room temperature. For example, with the total weight of 44.18 g ZnO and 2.82 g Ga_2O_3, we obtained a pellet of ZnO with Ga_2O_3 6 wt% with a diameter of 5 cm and a thickness of about 7 mm. The pellet was then sintered at 1,050°C for 3 hrs in atmosphere. The temperature profile is shown in Fig. 4.1. The obtained target looks like a white ceramic.

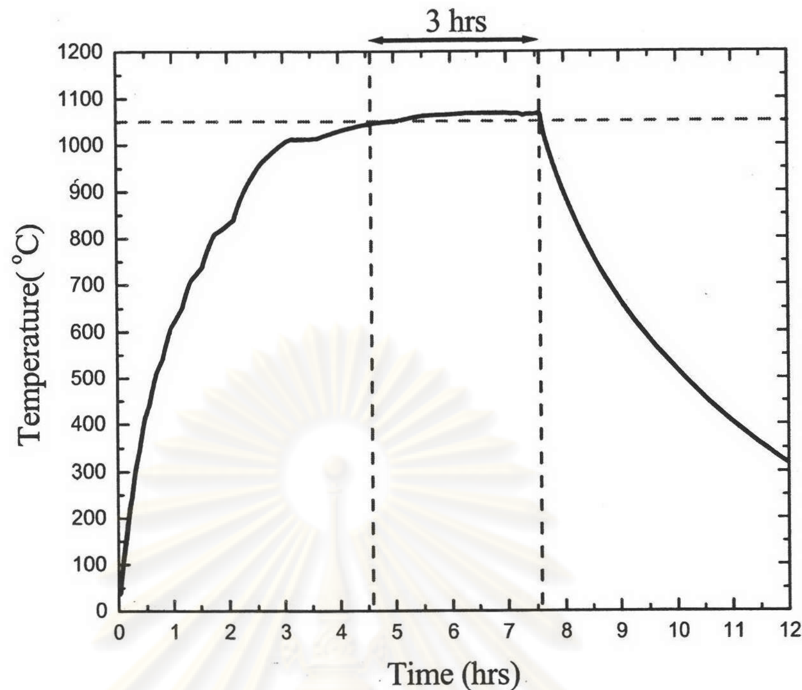

Figure 4.1: Temperature profile of the furnace preparing GZO target

In the final process, the sintered target must be polished for suitable thickness about 5.5 mm to fit into a sputtering gun. The ZnO pellets with Ga_2O_3 contents of 2, 3, 4 and 6 wt% were used as the targets for this research.

4.2 Substrate Preparation

Ga-doped ZnO thin films were deposited on 4.85×5.85 cm^2 soda-lime glass (SLG) substrates by RF magnetron sputtering. The soda-lime glass substrates were washed with soft sponge and detergent, and next ultrasonically cleaned in mixed detergent water, followed by DI-water and dried with nitrogen gas. The substrates were dipped into chromic acid for 10-12 hrs, and then they were ultrasonically cleaned again in pure DI-water, dried with nitrogen gas and finally baked at 70°C for 1 hr. The substrates were kept in a humidity-reduced container while they were not loaded into a sputtering system.

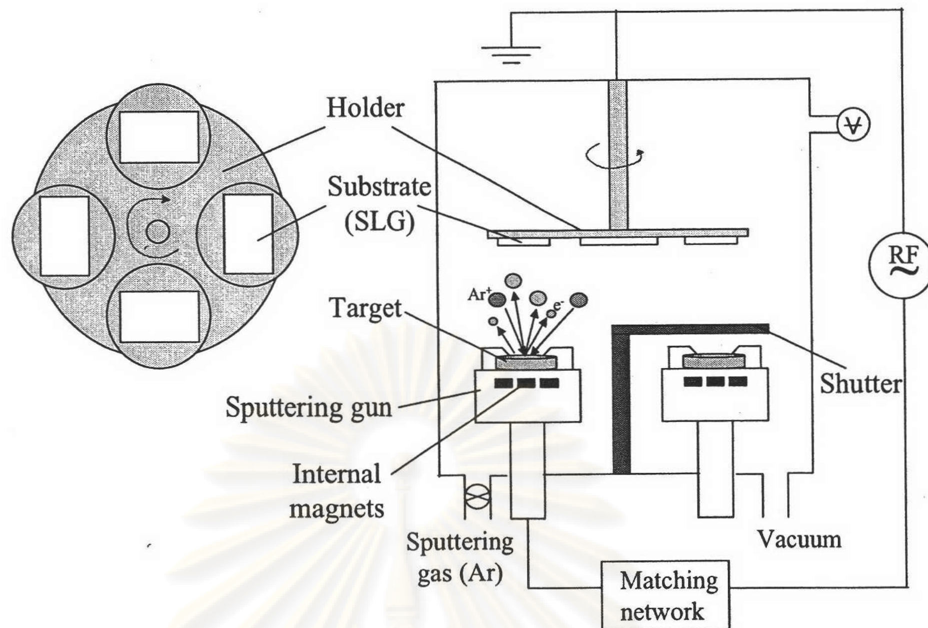

Figure 4.2: Schematic drawing of RF magnetron sputtering system

4.3 Preparation of Ga-doped ZnO Thin Films

The polished GZO target was loaded in the chamber of the sputtering system. The back side of the target was painted with thin silver paste and then clamped on the sputtering gun. The silver paste was used to achieve good thermal contact between the target and the sputtering gun to reduce the heat generated from the bombardment of particles on the target surface during sputtering.

Figure 4.2 shows the schematic diagram of the RF magnetron sputtering system used in this research, namely a planar sputtering. The SLG substrates were clamped with an aluminium holder, which was able to contain four substrates. The target-substrate distance was fixed at about 6.5 cm and the substrates were rotated parallel to the target surface. The shutter was placed between the target and the substrates in order to prevent undesirable sputtering. In our system, there are two sputtering guns but only one of them was used at a time. The sputtering gun can be switched to work by changing a cable of RF power supply.

In this system, a turbo molecular pump coupled with a rotary pump was used

Target -substrate distance	6.5 cm
Target diameter / thickness	5 cm / ~5.5 mm
Ga_2O_3 content in the target	2, 3, 4 and 6 wt%
Base pressure	$\leqslant 5.5 \times 10^{-6}$ mbar
Sputtering power	50 - 125 W
Sputtering pressure	6.0×10^{-3} - 1.0×10^{-2} mbar

Table 4.1: Deposition parameters for GZO thin films.

to achieve a pressure of an order of 10^{-6} mbar, (high vacuum). After the target was loaded completely and the pressure within chamber was reduced to 10^{-6} mbar, the target was first sputtered with 100 W power for 20 mins at 8.0×10^{-3} mbar of argon (Ar) gas pressure for surface cleaning. Before each deposition was started, the chamber was pumped down to the base pressure generally lower than 5.5×10^{-6} mbar. The surface of the target is usually pre-sputtered using the power of 100 W for 3 minutes in oxygen content of 4% (3.2×10^{-4} mbar) of overall sputtering gas pressure which was 8.0×10^{-3} mbar. The surface of the target became whiter after pre-sputtering due to the diffusion of oxygen atoms into the target. In other word, the surface of the target became more perfect ZnO structure due to the increasing oxygen atoms in lattice sites during pre-sputtering.

In order to reduce contamination of other gas species, we generally flush the chamber with Ar gas (8.0×10^{-3} mbar) for at least four times. After the surface of the target was improved, Ar gas was fed into the chamber. Next, the target was pre-sputtered before the deposition of the films using the power of 100 W in Ar pressure of 8.0×10^{-3} mbar for 5 min. Then, Ga-doped ZnO (GZO) thin films could be prepared by RF magnetron sputtering at a given working power and pressure while the substrates were rotated over the target. The planar sputtering was carried out at a power in the range 50-125 W and with a sputtering gas pressure of 8.0×10^{-3} mbar. In this work, the Ar gas pressure was also varied in the $6.0\times10^{-3}-1.0\times10^{-2}$ mbar range at a power of 100 W only to see the effect of the pressure of the sputtering gas. The deposition parameters are summarized in Table 4.1.

The planar sputtering was carried out at room temperature. The substrates were not heated intentionally. But because of the thermal radiation from the target and energy of the sputtered species, the substrates heated up during the deposition.

4.4 Characterization of Ga-doped ZnO Thin Films

4.4.1 Optical Characterization

Optical Transmission and Thickness Calculation

The optical transmission of GZO thin films were measured using a UV/VIS/UV spectrometer (Perkin Elmer model Lambda-900) in the wavelength ranging from 300 to 1500 nm. The Lambda-900 is a versatile spectrometer which can be operated in the ultraviolet, visible and near infrared ranges. The spectrometer features double-beams, double monochromators, and a ratio recording optical system. In other word, the reference beam and the sample beam can be detected simultaneously. The optical compartments are coated with silica for durability. The holographic gratings are used in each monochromator for the UV/VIS/NIR range.

The schematic diagram of the optical system is shown in Fig. 4.3. There are two radiation sources, a deuterium lamp (DL) and a halogen lamp (HL), cover the working wavelength range of the spectrometer. The operation of optical system can be described as the followings.

For operation in the near infrared (NIR) and visible (VIS) ranges, the radiation from halogen lamp is reflected from mirror M1 to mirror M2. At the same time, it blocks the radiation from the deuterium lamp. For operation in the ultraviolet (UV) range, mirror M1 is raised to permit radiation from the deuterium lamp to mirror M2.

Radiation from the respective source lamp is reflected from mirror M2 to mirror M3 through an optical filter on the filter wheel assembly (FW) to mirror

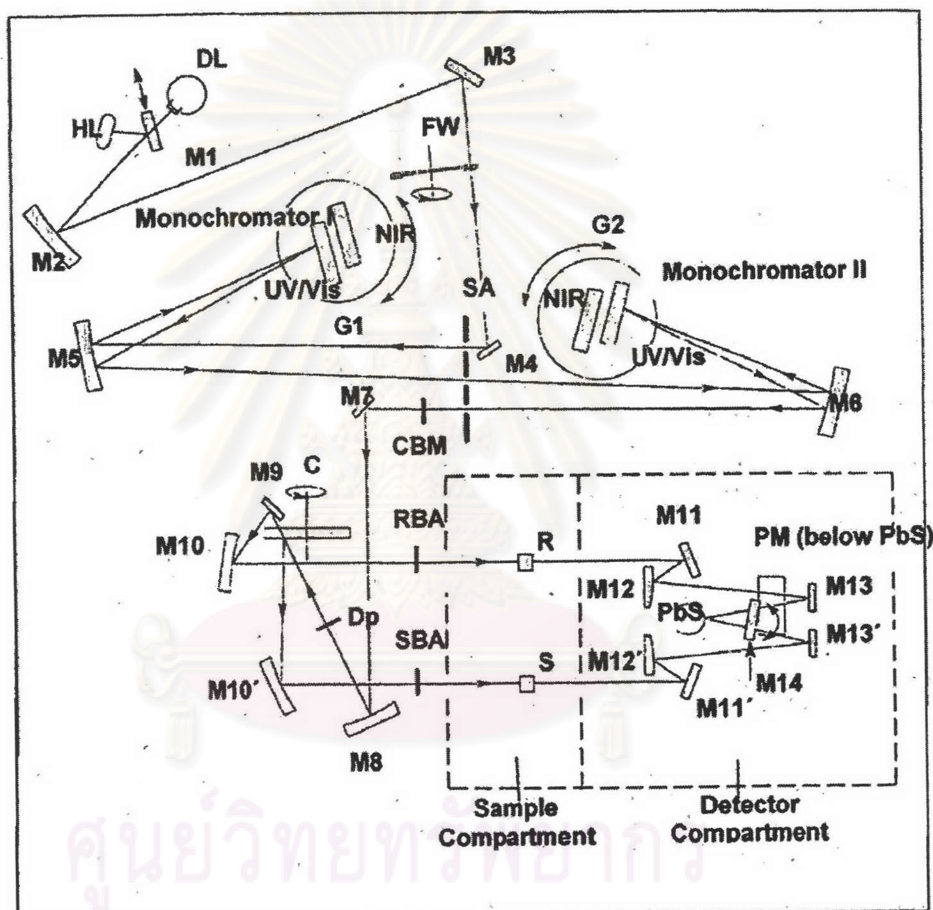

Figure 4.3: Schematic of optical system

ศูนย์วิทยทรัพยากร
จุฬาลงกรณ์มหาวิทยาลัย

M4. The radiation is reflected through the entrance slit of monochromator I, which collimates the radiation. The collimated radiation is reflected at the grating G1. Depending on the current wavelength range, the collimated radiation beam strikes either the UV/VIS grating or the NIR grating.

The radiation is dispersed at the grating to produce a spectrum. The rotational position of the grating effectively selects a segment of spectrum, reflecting this segment to mirror M5 and then through the exit slit serving as the entrance slit of Monochromator II. The radiation is reflected via mirror M6 to the grating on grating table G2 and then back via mirror M6 through the exit slit to mirror M7. The rotational position of grating table G2 is synchronized to that of G1. From mirror M7 the radiation beam is reflected via mirror M8 to the chopper assembly (C).

The chopper separates the radiation into two beams. As the chopper rotates, especially, a mirror segment and a window segment, are brought alternately into the radiation beam. When a window segment enters the beam, radiation passes through to mirror M9 and is then reflected via mirror M10 to create the reference beam (R). On the other hand, when a mirror segment enters, the beam of radiation is reflected via mirror M10′ to form the sample beam (S).

In the sample compartment, a clean blank soda-lime glass is used as a reference substrate and the sample is GZO thin film coated on one side of the soda-lime glass. The radiation beams passing alternatively through the sample and a reference SLG are reflected by mirror M11, M12, M13 and M11′, M12′, M13′ of the optics in the detector assembly. Mirror M14 is rotated to select the appropriate detector. A photomultiplier (PM) is used in the UV/VIS range while a lead sulfide (PbS) detector is used in the NIR range.

The optical transmission of the films were measured in the percent of the ratio of intensity of the sample beam to the reference beam as shown in Fig. 4.4. The incoming beam is incident normally on the surface of the sample and the reference glass. The detectors measured intensity of transmitted beam (I_t and I_0), and the

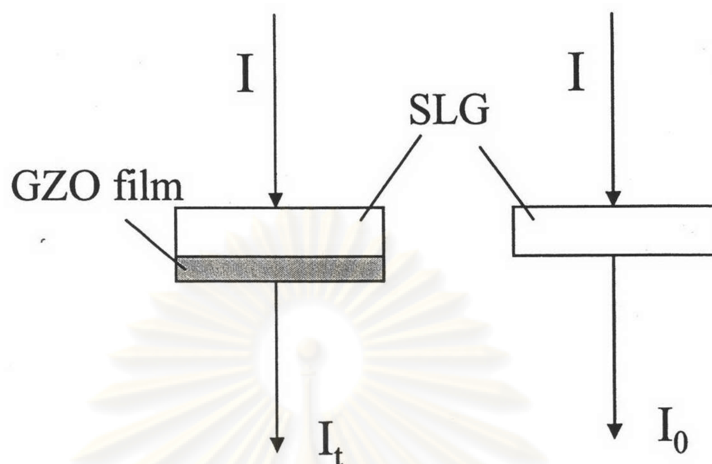

Figure 4.4: Schematic drawing of optical transmission measurement

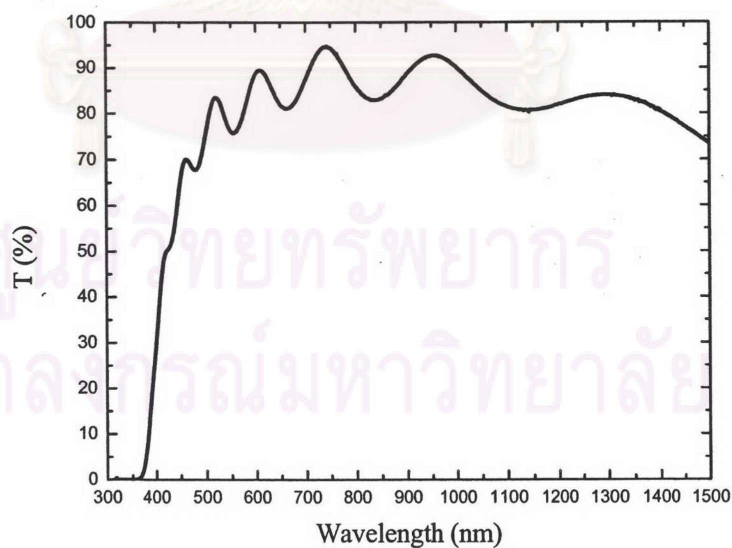

Figure 4.5: Optical transmission of the GZO film as a function of wavelength

percent of optical transmission can be expressed as

$$T(\%) = \frac{I_t}{I_0} \times 100. \tag{4.1}$$

A typical optical transmission spectrum of GZO thin film is shown as an example in Fig. 4.5. All samples have smooth surfaces, and the transmission spectrum shows interference fringes with deep valleys and tall crests. The fringes result from the interference of waves due to the thickness of the film coated on the substrate.

The thickness of thin film (d) can be calculated from two maxima (or two minima) positions in the spectrum according to

$$d = \frac{M\lambda_1\lambda_2}{2n\left|\lambda_2 - \lambda_1\right|}, \tag{4.2}$$

where M is the number of oscillations between the two extrema (maxima or minima) occurring at λ_1 and λ_2, and n is index of refraction of GZO thin film. In this research, we use $n = 2.02$ for the GZO thin film [25, 31].

Optical Absorption Coefficient Calculation

The optical absorption coefficient (α') that related to the intensity of the reference beam (I_0), the intensity of the transmission beam from the sample (I_t) and the film thickness (d) can be expressed as

$$\alpha' = \frac{1}{d}\ln(\frac{I_0}{I_t}). \tag{4.3}$$

From Eq. 4.1, we obtain

$$\alpha' = \frac{1}{d}\ln(\frac{100}{T}), \tag{4.4}$$

where T is a percentage of optical transmission of thin film at the wavelength λ.

Since the obtained thin films are polycrystalline, they have some defects in the crystal structure, the background absorption coefficient (α_0) will be obtained. The α_0 is a constant in the range of photon energy being less than energy gap (E_g) of thin film. The electrons cannot cross the energy gap from the valence band to

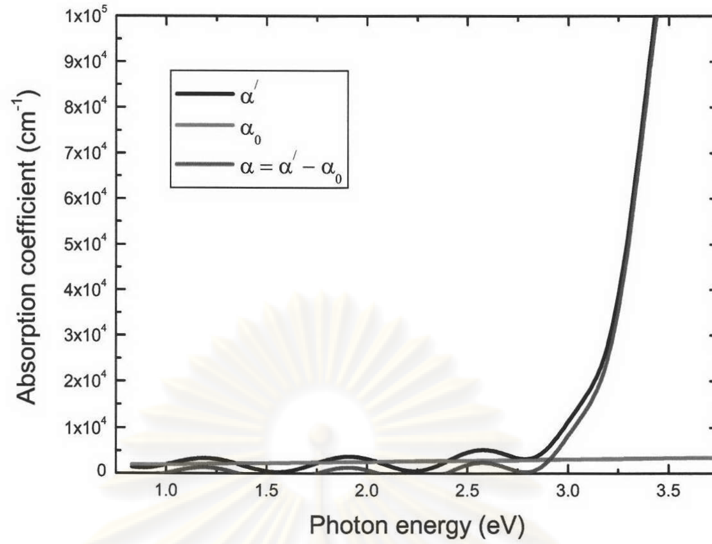

Figure 4.6: Optical absorption coefficient of GZO thin film as a function of photon energy

the conduction band. Therefore, the α_0 does not relate to E_g and the α_0 must be subtracted from α' in order to obtain the value of real optical absorption coefficient (α) relating to energy gap. It can be expressed as

$$\alpha = \alpha' - \alpha_0. \tag{4.5}$$

By plotting absorption coefficient vs. photon energy, a straight-line averaging the oscillated absorption coefficient in the low photon energy region is drawn to the high photon energy region, as shown in Fig. 4.6. The optical absorption coefficient (α) is obtained for determining of energy gap (E_g) of thin film.

Energy Gap Determination

For interband transition of semiconductor that has a direct band gap, the relation between the energy gap and the optical absorption coefficient is [32]

$$\alpha h\upsilon = A(h\upsilon - E_g)^{\frac{1}{2}}, \tag{4.6}$$

where A is a constant, h is the Plank's constant, and υ is the frequency of the radiation. By determining α from the measured optical transmission spectrum and

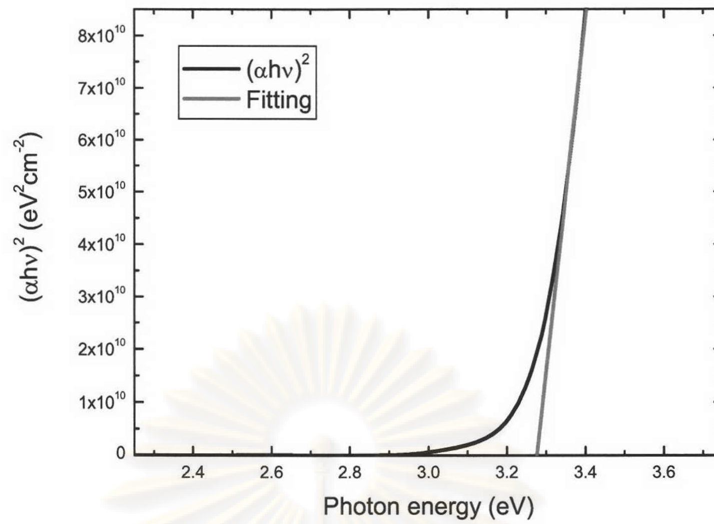

Figure 4.7: Plot of $(\alpha hv)^2$ vs. photon energy for GZO thin film

by plotting $(\alpha hv)^2$ vs. hv, where hv is the photon energy, the optical energy gap can then be obtained from the intercept of graph for direct allowed transition. The photon energy at the point where $(\alpha hv)^2 = 0$ is the energy gap of which value is determined by the extrapolation method. The extrapolation of the linear segment of the spectrum or curve towards the x-axis gives the value of energy gap. Figure 4.7 shows the calculation for the GZO thin film of which energy gap is about 3.28 eV.

4.4.2 Electrical Characterization

The electrical resistivity, Hall mobility and carrier concentration were measured by Hall measurement using the Van der Pauw technique, which is the four-point probe method. The samples were wired up with the copper wires and silver paste. The four probes were contacted onto the corners of the film surface. Each contact was labeled with the number 0 to 3. The Hall effect measurement control system applied the high-voltage constant current to the sample. In addition, the system also controlled the direction of the applied magnetic field for the determination of Hall mobility. Figure 4.8 shows the contacts of the sample used to apply the current and measure

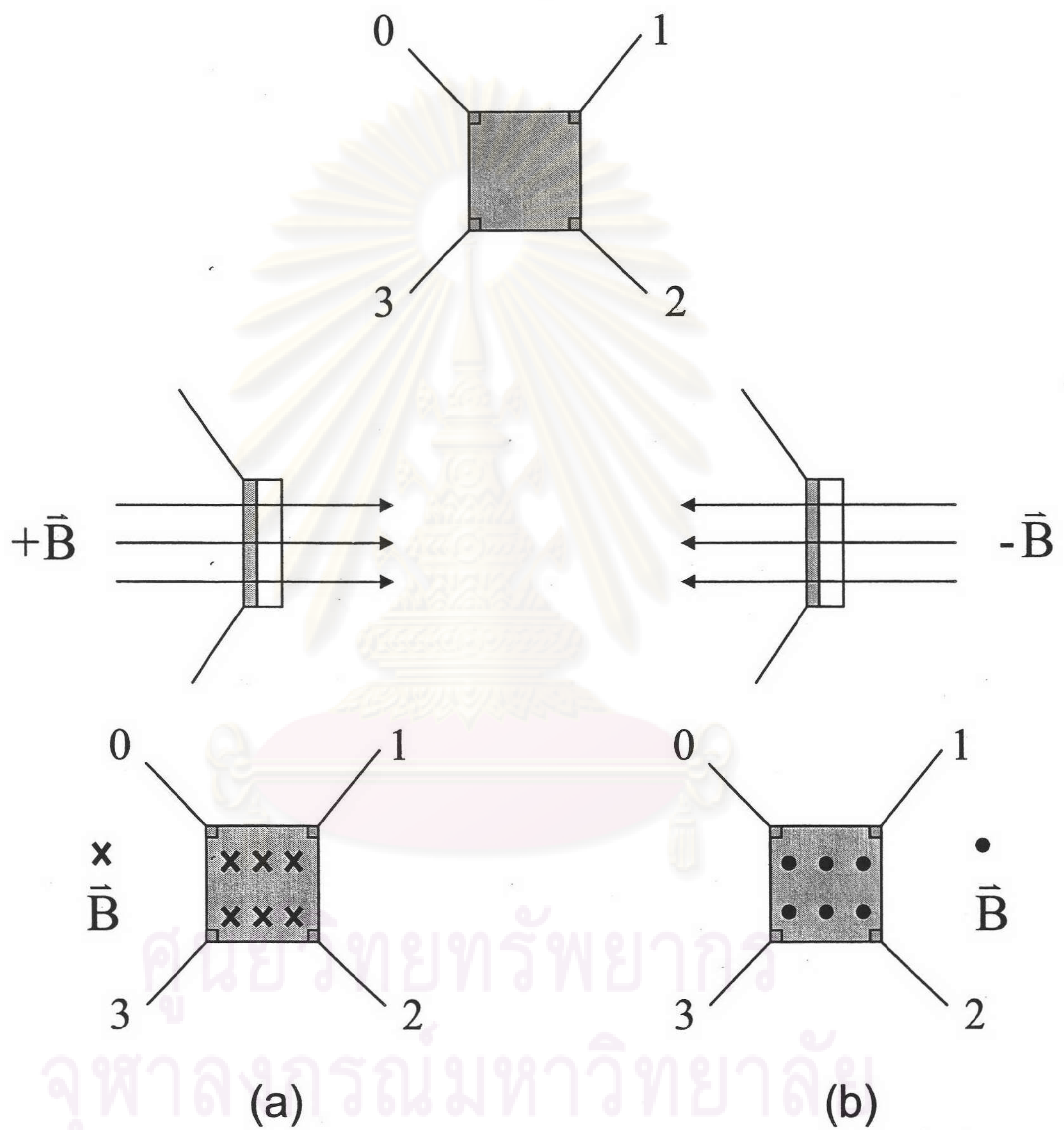

Figure 4.8: The electrical measurement using the four point probe method

ศูนย์วิทยทรัพยากร
จุฬาลงกรณ์มหาวิทยาลัย

(a) forward current

Configuration	I+	I-	V+	V-	Measurement parameters
1	I_1	I_2	V_3	V_0	I_{12} , V_{30}
3	I_2	I_3	V_0	V_1	I_{23} , V_{01}
5	I_3	I_0	V_1	V_2	I_{30} , V_{12}
7	I_0	I_1	V_2	V_3	I_{01} , V_{23}

(b) reverse current

Configuration	I+	I-	V+	V-	Measurement parameters
2	I_2	I_1	V_3	V_0	I_{21} , V_{30}
4	I_3	I_2	V_0	V_1	I_{32} , V_{01}
6	I_0	I_3	V_1	V_2	I_{03} , V_{12}
8	I_1	I_0	V_2	V_3	I_{10} , V_{23}

Table 4.2: Configuration of electrical resistivity measurement by the following applied current

(a) forward current

Configuration	I+	I-	V+	V-	Measurement parameters
9, 13, 17	I_1	I_3	V_2	V_0	I_{13} , V_{20}
11, 15, 19	I_2	I_0	V_1	V_3	I_{20} , V_{13}

ศูนย์วิทยทรัพยากร
จุฬาลงกรณ์มหาวิทยาลัย

(b) reverse current

Configuration	I+	I-	V+	V-	Measurement parameters
10, 14, 18	I_3	I_1	V_2	V_0	I_{31} , V_{20}
12, 16, 20	I_0	I_2	V_1	V_3	I_{02} , V_{13}

Table 4.3: Configuration of Hall mobility measurement by following applied current

the voltage using all possible configurations of the measurement. The magnetic field was not applied to a sample during the measurement of electrical resistivity. For Hall mobility measurement, the magnetic field was applied in the direction of forward ($+\vec{B}$) and reverse ($-\vec{B}$), as shown in Fig. 4.8a and b, respectively. The system measured and recorded all data in 20 configurations, as shown in Tables 4.2 and 4.3. The electrical resistivity and Hall mobility were calculated from the measurement in the configurations 1-8 and 13-20, respectively.

The configurations 9-12 were used for the Hall mobility measurement without applied magnetic field, while the configurations 13-16 and 17-20 were used for the measurement of Hall mobility with the forward magnetic field ($+\vec{B}$) and reverse magnetic field ($-\vec{B}$), respectively. The resistivity and Hall mobility were obtained from the calculation using Van der Pauw technique. The resistivity (ρ) is proportional to the inverse of product of carrier concentration (n) and mobility (μ) as

$$\rho = \frac{1}{q\mu n}, \tag{4.7}$$

where q is the electronic charge. As a result, the carrier concentration can be determined from Eq. 4.7.

4.4.3 Structural Characterization

The structural properties such as the crystallinity and crystal orientation of the GZO films were determined by the X-Ray diffraction (XRD) using a Bruker AXS (D8 Advance) diffractometer with Cu-K_α radiation (λ = 1.5405Å). The XRD pattern was scanned from 2θ =33.0° to 35.5° with a scan step of 0.015° using detection time of 3 s per step. The current and voltage of the system were set at 30 mA and 40 kV, respectively. A sample was rotated with the degree of θ while the X-ray detector moved with 2θ corresponding to Bragg's law. The XRD pattern of the films shows the dependence of the intensity of diffraction on different positions of 2θ. Figure 4.9 shows the XRD pattern in the wide range of GZO thin film prepared by using different Ga_2O_3 content and sputtering conditions. It was

clearly seen that there was a dominant peak at $2\theta \approx 34°$ in all patterns, then the above range of scanning was used to study the crystal structure of the films in this research.

The experimental procedure can be concluded into the flow chart as shown in Fig. 4.10.

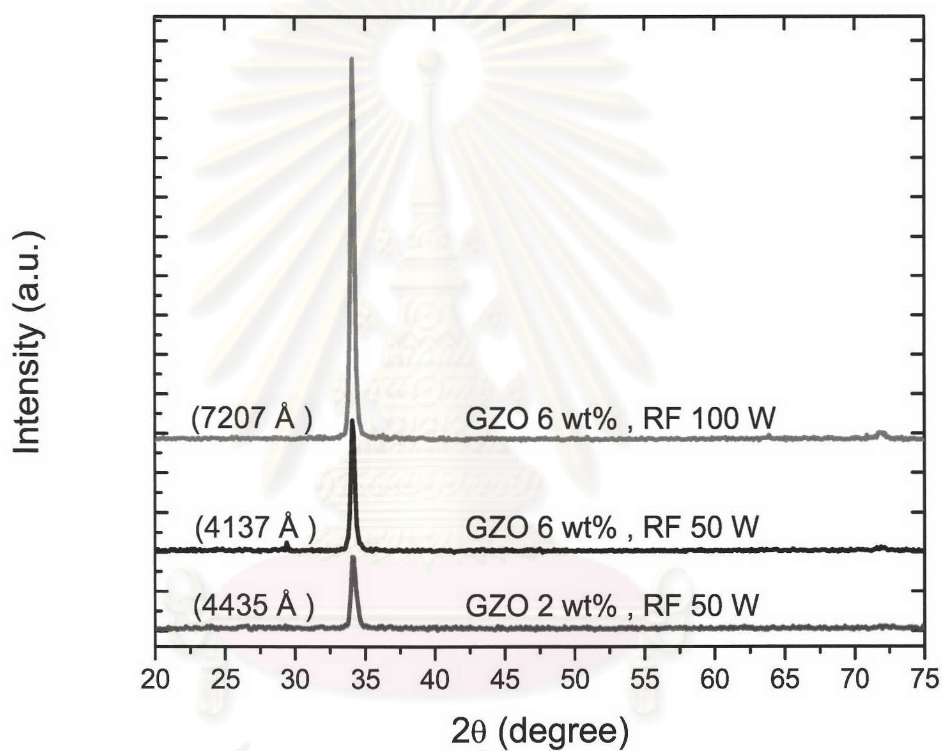

Figure 4.9: XRD patterns of GZO thin films deposited at different dopings and sputtering conditions

ศูนย์วิทยทรัพยากร
จุฬาลงกรณ์มหาวิทยาลัย

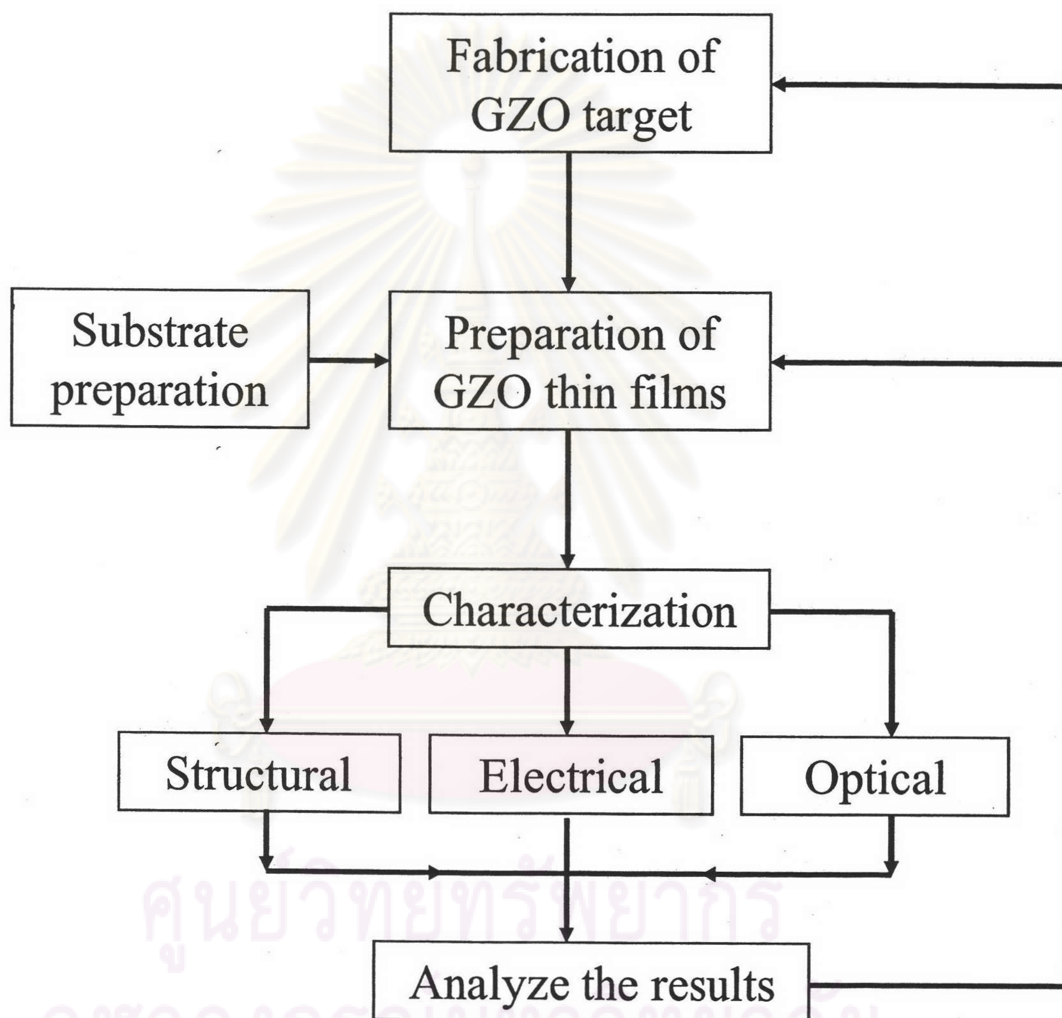

Figure 4.10: The flow chart of experimental procedure

ศูนย์วิทยทรัพยากร
จุฬาลงกรณ์มหาวิทยาลัย